

X-RAY CHERENKOV RADIATION AS A SOURCE FOR RELATIVISTIC CHARGED PARTICLE BEAM DIAGNOSTICS

JAI
John Adams Institute for Accelerator Science

Royal Holloway
University of London

A.S. Konkov, A.S. Gogolev, A.P. Potylitsyn, Tomsk Polytechnic University
P.V. Karataev, John Adams Institute at Royal Holloway, University of London



IBIC 2013
International Beam Instrumentation Conference

INTRODUCTION

Recent progress in development of accelerator technology for future linear colliders and X-ray free electron lasers has generated an interest in developing novel diagnostics equipment with resolution overpassing the unique beam parameters. Monitors based on backward transition and synchrotron radiation have proved their feasibility. However, the developed techniques are either applicable for a single facility or their accuracy is limited. Thus it is necessary to develop novel methods with a wider application range. The most promising techniques are based on polarization radiation.

Polarization radiation appears when due to dynamic polarization of atomic electron shells of a medium by the self electric field of a charged particle moving rectilinearly and with constant velocity. Depending on the conditions of the particle motion in the medium (or in its vicinity) here are different types of polarization radiation generated: Vavilov-Cherenkov radiation (CR), transition radiation (TR), diffraction

radiation (DR), Smith-Purcell Radiation (SPR), etc. One should note that DR and SPR are more preferable for developing non-invasive methods of charged particle beam diagnostics, because generating the radiation the particle beam does not directly interact with the target, and, therefore, the trajectory perturbation will be minimal.

CR in X-ray region in the vicinity of the absorption edges is one of the promising sources. In [1] the authors represented the first prediction of the phenomenon. The authors have demonstrated that passing through a plate of finite thickness an ultrarelativistic charged particle generates CR which intensity significantly over passes the TR intensity generated from the surface of the plate. Later on, the authors of [2-4] have demonstrated that CR can be generated by moderately relativistic electrons as well.

In this work we used the method of "polarization currents" [5] to determine the CR characteristics generated by a charged particle at oblique incidence through a plate of finite dimensions and finite conductivity in the vicinity of the atomic absorption edges.

FEATURES OF X-RAY CR

It is well known that the Cherenkov radiation (CR) is generated by charged particle moving in a medium rectilinearly and with constant velocity, which magnitude is larger than the phase velocity of light inside that medium. The radiation has a continuous spectrum and specific angular distribution. The characteristic angle, Θ , of the emitted radiation with respect to the particle trajectory, \mathbf{v} , is defined by $n\beta \cos \Theta = 1$, where n is refractive index of the transparent medium. Typically in X-ray wavelength range the CR condition cannot be fulfilled because for all materials the refractive index is smaller than unity. However, in [1] the authors demonstrated that in the vicinity of the absorption edges the real and imaginary parts of dielectric permittivity experience a resonant increase (see, for instance, Fig. 1). As a result the real part of the refractive index experiences a resonant increase reaching values above unity. In this case the CR condition can be fulfilled and an X-ray CR can be emitted in a very narrow spectral range with bandwidth of order of 1 – 1.5 eV. In this paper we consider the CR in the vicinity of the absorption edges of carbon. Fig. 1 illustrates the dependence of real and imaginary parts of $\epsilon(\omega) = 1 - \delta(\omega) - i\eta(\omega)$ – the dielectric permittivity versus the photon energy calculated for amorphous carbon using [6]. The calculation of the CR characteristics using the method of polarization currents was performed using the geometry shown in Fig. 2. A particle with charge e , moving with constant velocity β , incident with an angle α on a plate of thickness d . Due to dynamic polarization of the target medium both transition and Cherenkov radiation is emitted along the direction z and characterised by polar θ and azimuthal ϕ observation angles.

Due to the azimuthal symmetry the dependence on ϕ is absent. One can see that in contrast to the TR (TR peak at $\theta = \pm\gamma^{-1} = \pm0.26^\circ$) the CR intensity (radiation peak at $\theta = \pm4^\circ$) grows quadratically as a function of the target thickness. Moreover, at some thickness the CR intensity significantly exceeds the TR intensity. The X-ray CR is very sensitive to the

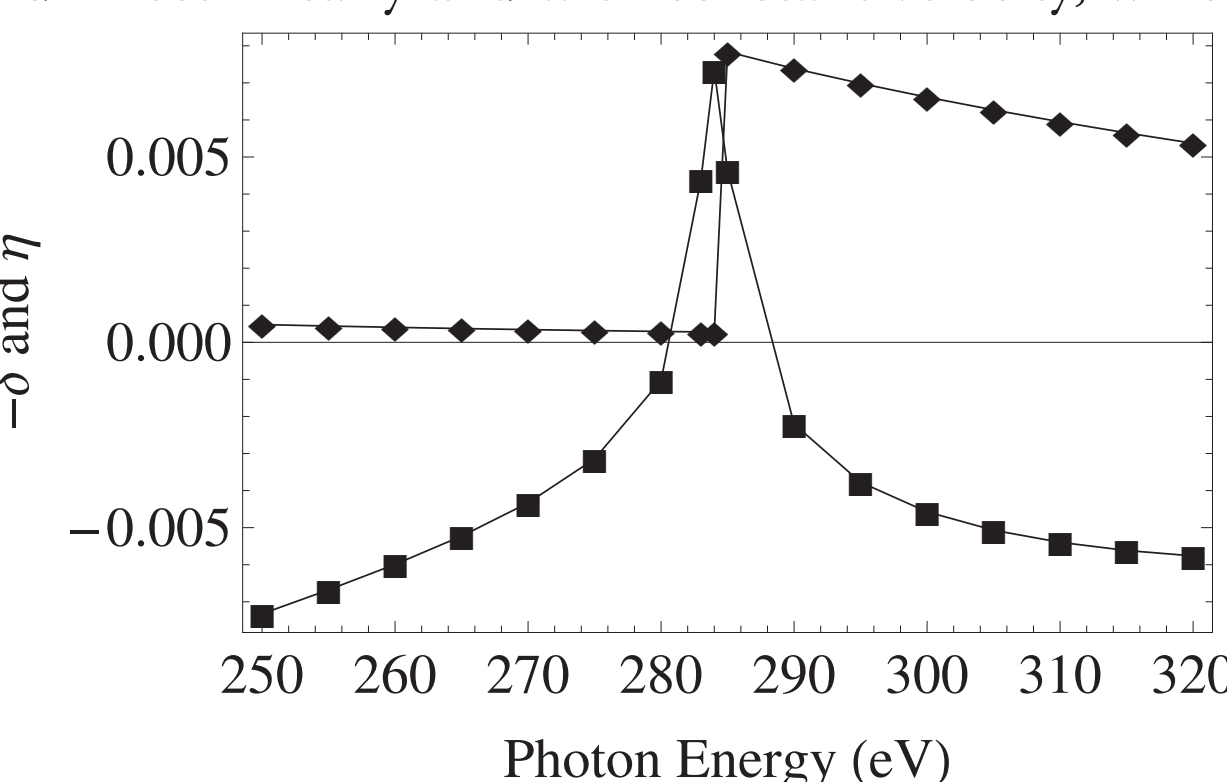


Figure 1: Dependence of the real ($-\delta$) and imaginary (η) parts of dielectric permittivity of amorphous carbon in the vicinity of the K-absorption edge (284 eV). Both real (\blacksquare), and imaginary (\diamond) parts experience a resonant increase at the photon energy of $E_{ph} = 284$ eV.

Figure 2: The calculation geometry

with charge e , moving with constant velocity β , incident with an angle α on a plate of thickness d . Due to dynamic polarization of the target medium both transition and Cherenkov radiation is emitted along the direction z and characterised by polar θ and azimuthal ϕ observation angles.

Due to the azimuthal symmetry the dependence on ϕ is absent. One can see that in contrast to the TR (TR peak at $\theta = \pm\gamma^{-1} = \pm0.26^\circ$) the CR intensity (radiation peak at $\theta = \pm4^\circ$) grows quadratically as a function of the target thickness. Moreover, at some thickness the CR intensity significantly exceeds the TR intensity. The X-ray CR is very sensitive to the

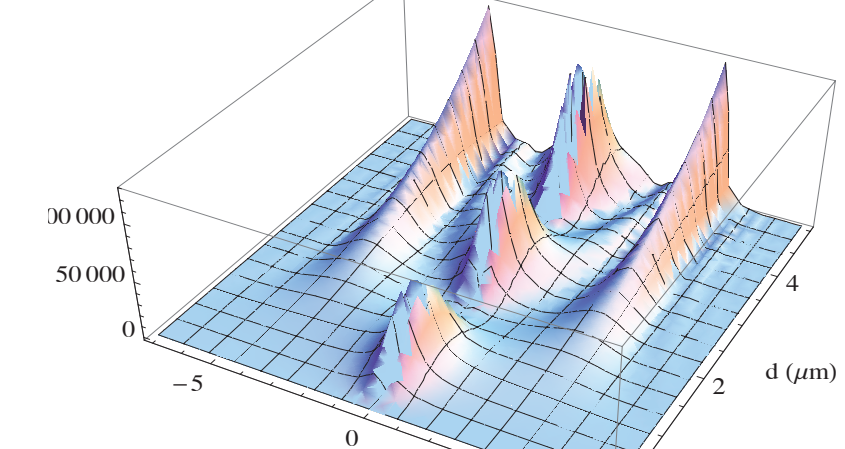


Figure 3: Dependence of the PR intensity as a function of the polar observation angle θ and the target thickness d . Parameters: $\gamma = 240$, $\alpha = 0$, $h\omega = 284$ eV, $\phi = \pi$.

CONCLUSION

In this paper we have demonstrated a new model for calculating polarization characteristics in X-ray frequency range from a target of an arbitrary shape and arbitrary dielectric permittivity. For calculations we used a recently developed method of polarization currents. We have demonstrated CR characteristics in X-ray region significantly depends on the energy of the emitted photons, because the CR is only generated in the frequency region in the vicinity of the atomic absorption edges. This peculiarity can be explained by resonance behavior of the permittivity in the given frequency range. Because of strong non-linear dependence of the photon yield on the photon energy, the CR in the vicinity of the absorption edge is highly monochromatic. The CR photon yield is comparable, and for many cases significantly higher, than the TR photon yield. For the moderate relativistic energies $\gamma < 100$, the variation of the energy significantly influences the CR characteristics. Such peculiarity can be used to diagnose the beam energy via the analysis of the special-spectral distribution shape and intensity. In the vicinity of moderate relativistic energies one can increase the CR intensity by increasing the angle of incidence. However, increasing the charged particle beam energy the spectral angular CR density becomes very sensitive to the angle of the particle incidence. Such peculiarity can be used to diagnose the particle beam angular divergence. One should notice that in the vicinity of particle energies of order of $\gamma \sim 10$, CR and TR interfere. The visibility of the interference fringe pattern depends on the spatial coherency of the radiation. The spatial coherency depends on the transverse dimension of the particle beam. Summarizing the analysis the peculiarities of the CR in the vicinity of the absorption edges open a wide range of possibilities for charged particle beam diagnostics. Nevertheless, the model is still under analysis. A more detailed proposal devoted to the diagnostics will be presented later.

THEORETICAL APPROACH

The theoretical approach is based on the method of polarization currents. The field of the Polarization Radiation (PR) emitted by medium atoms excited (polarised) by the external field \mathbf{E}^0 of the passing particle with energy $\gamma = \frac{E}{mc^2} = \frac{1}{\sqrt{1 - \beta^2}}$ moving rectilinearly and with constant velocity $v = \beta c$ in a substance (or in its vicinity) can be represented as a solution of "vacuum" macroscopic Maxwell equations. For a non-magnetic medium the density of the polarization currents in a right hand side of the equations can be written as

$$\mathbf{j}_{pol} = \sigma(\omega)(\mathbf{E}^0 + \mathbf{E}^{pol}(\mathbf{j}_{pol})) \quad (1)$$

where $\mathbf{E}^0 = \mathbf{E}^0(\mathbf{r}, \omega)$ and $\mathbf{E}^{pol} = \mathbf{E}^{pol}(\mathbf{r}, \omega)$ – are the Fourier Image of the particle filed in vacuum and the field generated by the currents induced in the medium. The medium conductivity, $\sigma(\omega)$, is related to the dielectric permittivity $\epsilon(\omega)$ as

$$\sigma(\omega) = \frac{i\omega}{4\pi}(1 - \epsilon(\omega)) \quad (2)$$

Solving the Maxwell equations in a wave-zone for a target of finite volume V_T one can derive an expression for magnetic field, \mathbf{H}^{pol} , of the polarization radiation emitted by the medium atoms excited by the passing particle filed in the form

$$\mathbf{H}^{pol}(\mathbf{r}, \omega) = \text{curl} \frac{1}{c} \int_V \sigma(\omega) \mathbf{E}^0(\mathbf{r}', \omega) \frac{\exp(i\sqrt{\epsilon(\omega)}|\mathbf{r}' - \mathbf{r}|/\omega/c)}{|\mathbf{r}' - \mathbf{r}|} d^3 r'. \quad (3)$$

Here we assume the energy loss by the particle is negligibly small in comparison to its total energy. One should note that the Eq. (3) is an exact solution of Maxwell equations, which allows us to avoid solving the integral equation (1). When we took into account the second term in Eq. (1), the wave number ω/c in vacuum was simply replaced by $\sqrt{\epsilon(\omega)}\omega/c$. Such replacement describes the "renormalization" of the particle field inside the medium due to the field of the polarization currents[5]. Despite of a simple form the Eq. (3) describes all types of polarization radiation generated in a medium of an arbitrary conductivity and arbitrary inhomogeneity (i.e. in a target of an arbitrary shape), which is the main advantage of the method.

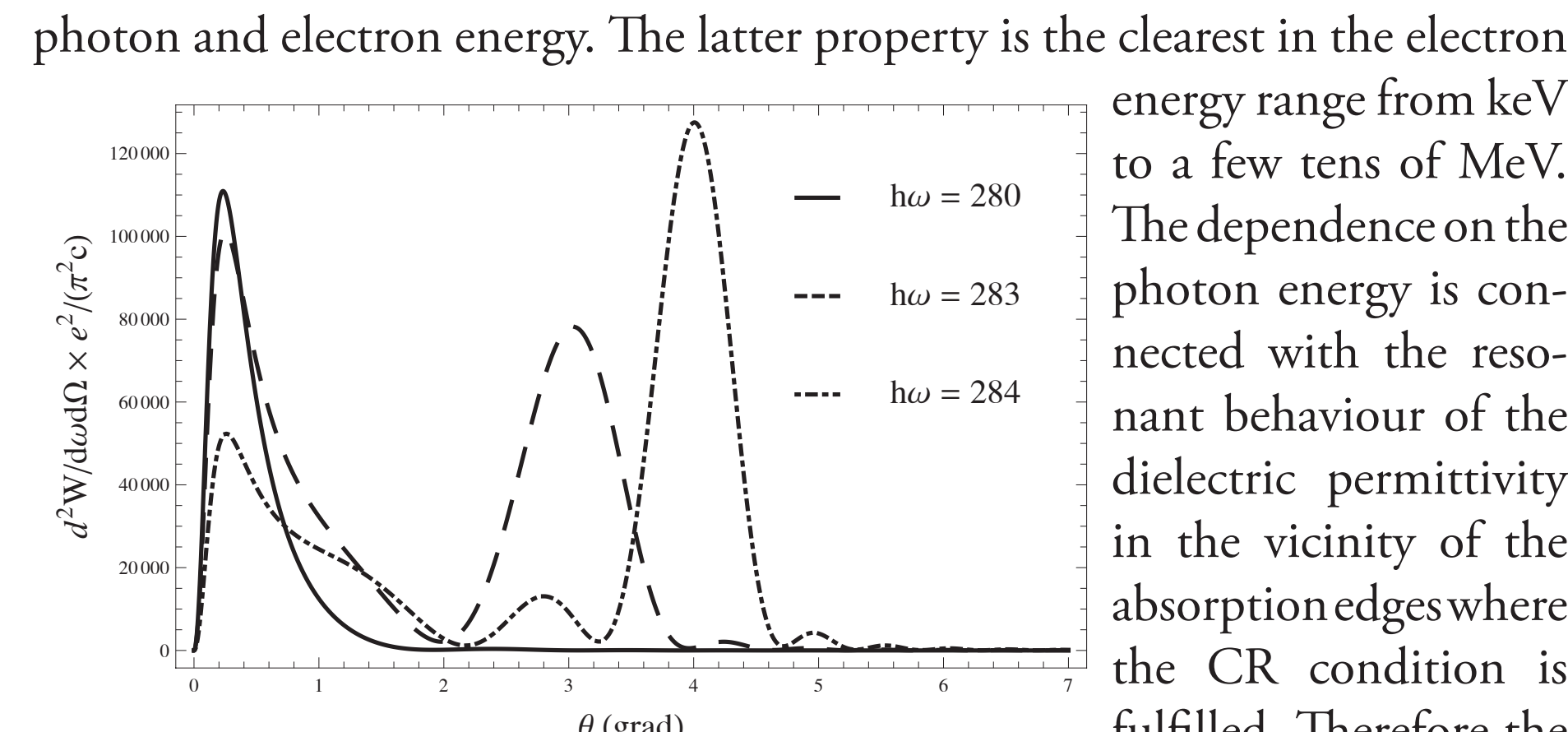


Figure 4: Dependence of the CR intensity versus polar observation angle θ for different photon energies. Parameters: $\gamma = 240$, $\alpha = 0$, $d = 5$ μm, $\phi = \pi$.

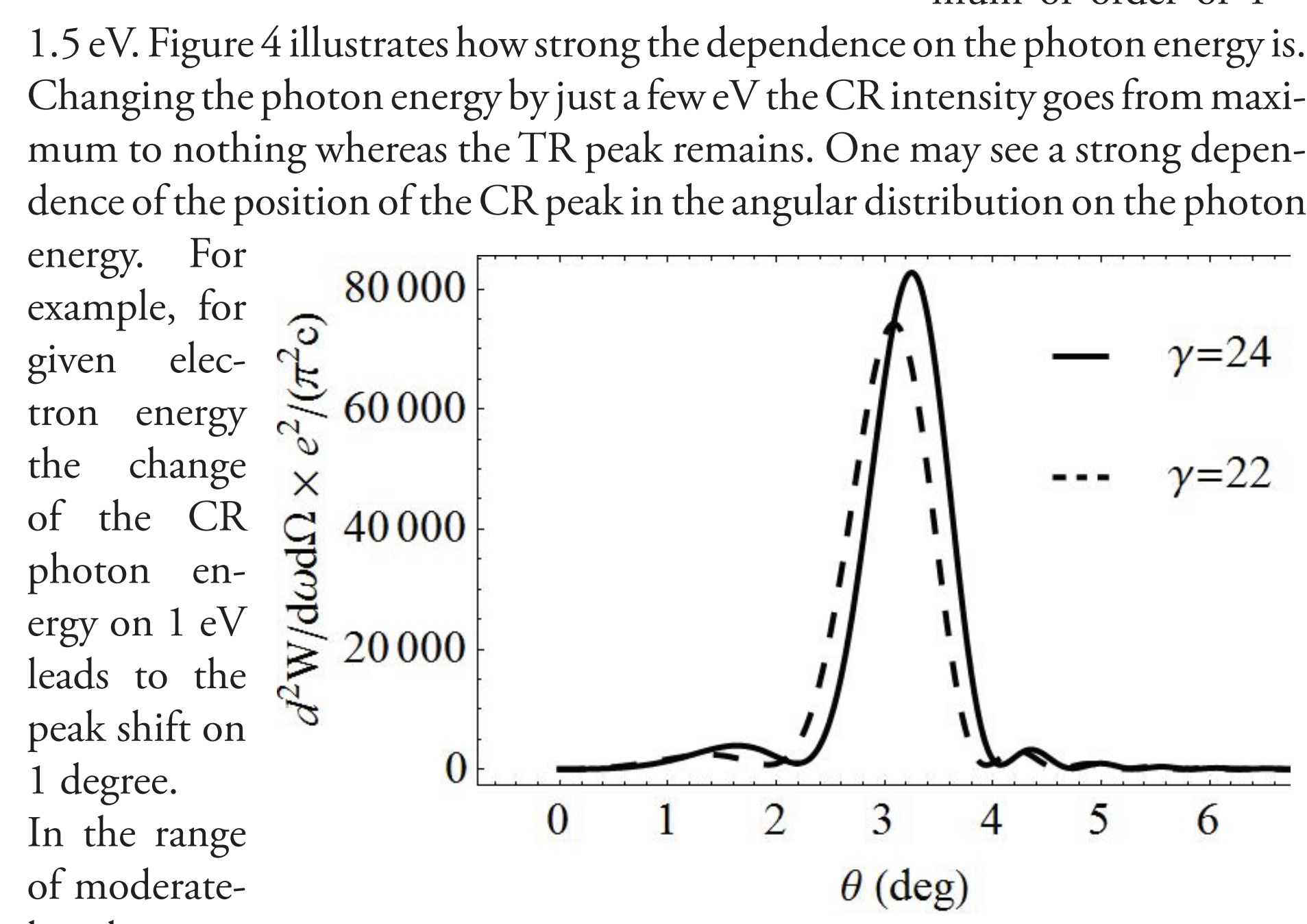


Figure 5: Dependence of the radiation intensity on the polar observation angle θ for different electron energies. Parameters: $\alpha = 0$, $d = 5$ μm, $h\omega = 284$ eV, $\phi = \pi$.

One should notice that in the area of moderate relativistic energies of charged particles the CR intensity significantly surpasses the TR intensity when increasing the angle α (see, for instance, Fig. 8). However, for higher particle energy ($\gamma > 100$), even a small change in the particle incidence angle leads to appearance of a strong asymmetry of angular distribution and the TR intensity significantly surpasses the CR intensity (see Figs. 8 and 9).

At lower energies the CR and TR interfere with each other. As a result the shape of the TR distribution acquire an oscillatory behavior with maximum intensities growing with the target thickness because of the CR contribution (see Fig. 6).

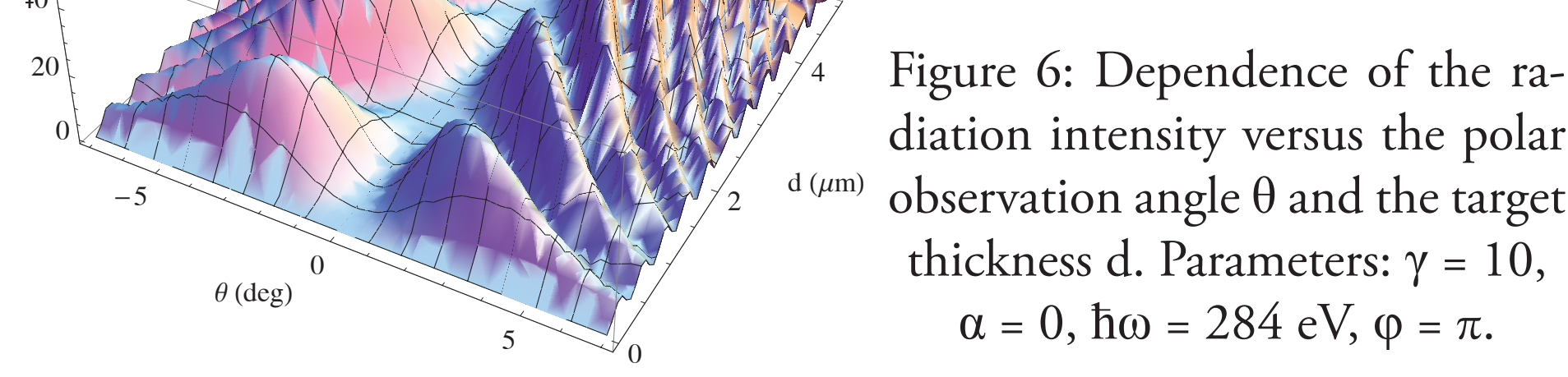


Figure 6: Dependence of the radiation intensity versus the polar observation angle θ and the target thickness d . Parameters: $\gamma = 10$, $\alpha = 0$, $h\omega = 284$ eV, $\phi = \pi$.

Figure 7 illustrates the dependence of the spectral-angular radiation density as a function of the observation angles. When the angle of incidence $\alpha \neq 0$, there appears an azimuthal asymmetry which leads to deformation of both TR (internal cone) and CR (external cone) angular distributions. When the angle of incidence increases, the degree of azimuthal asymmetry increases. The radiation distribution is squeezed along the direction characterised by the angle $\phi = \pi$ with non-uniform distribution of the energy along the polar observation angle.

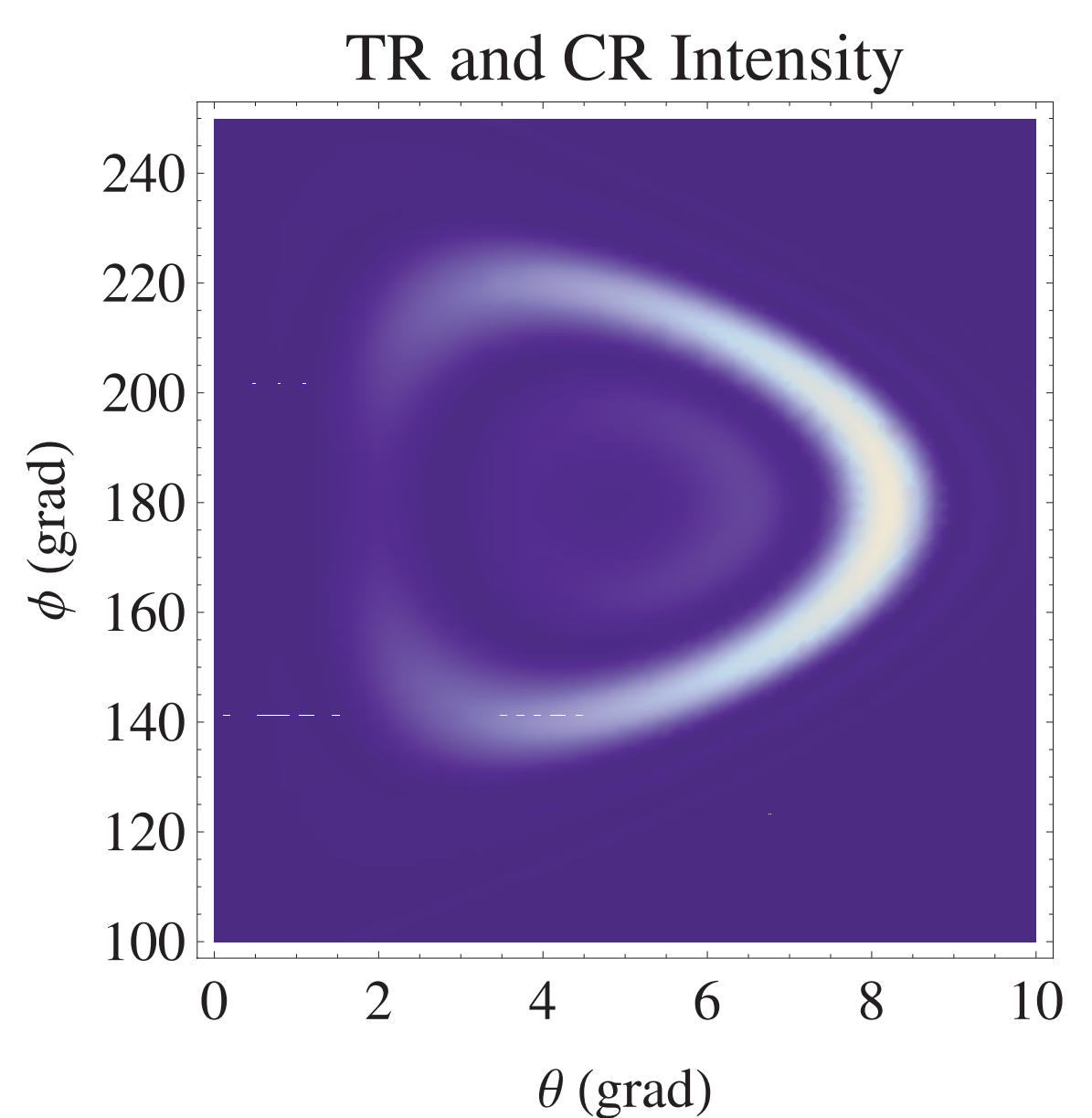


Figure 7: Dependence of the polarization radiation intensity versus the observation angles. Parameters: $\gamma = 24$, $\alpha = 5^\circ$, $h\omega = 284$ eV, $d = 5$ μm.

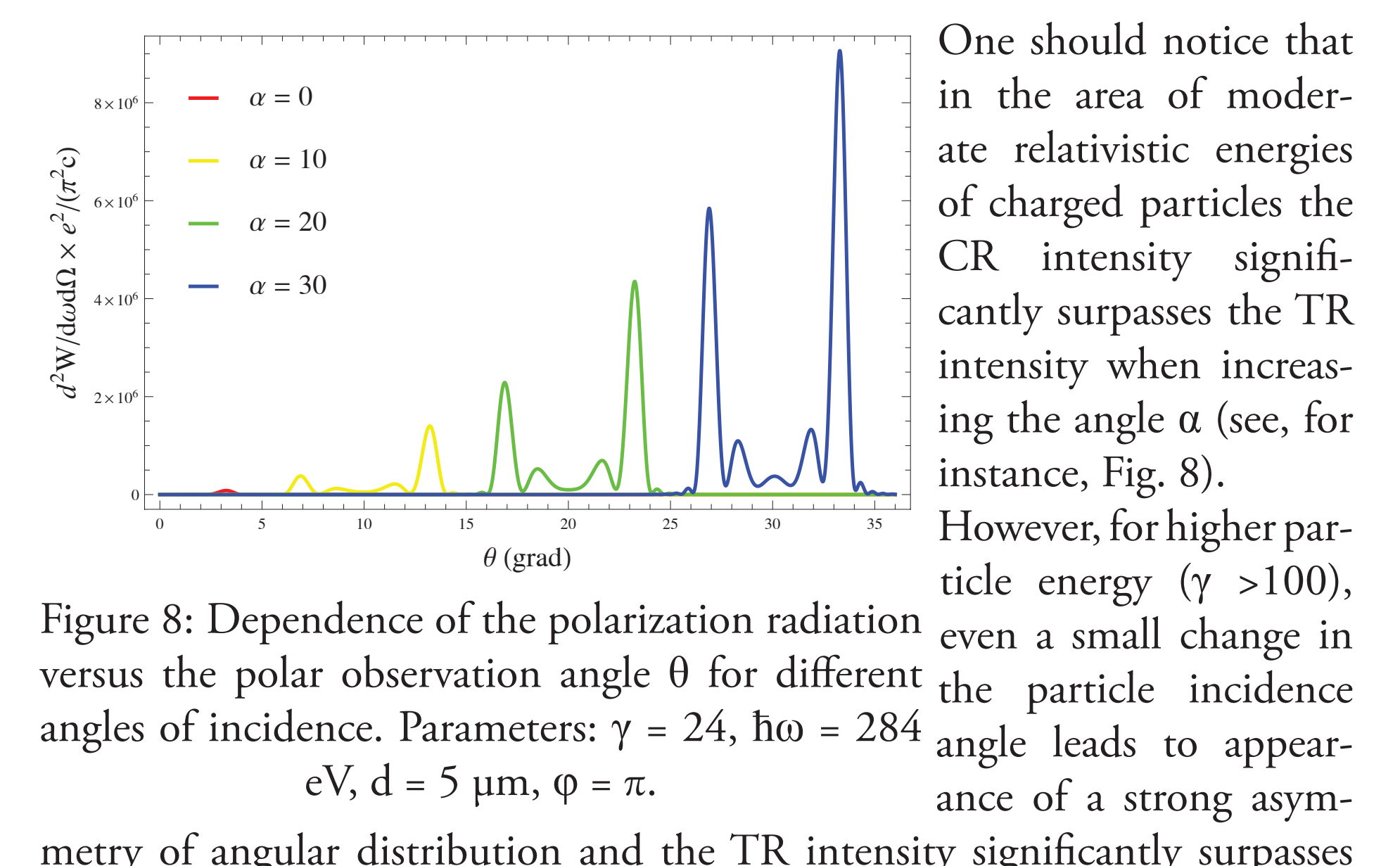


Figure 8: Dependence of the polarization radiation intensity versus the polar observation angle θ for different angles of incidence. Parameters: $\gamma = 24$, $h\omega = 284$ eV, $d = 5$ μm, $\phi = \pi$.

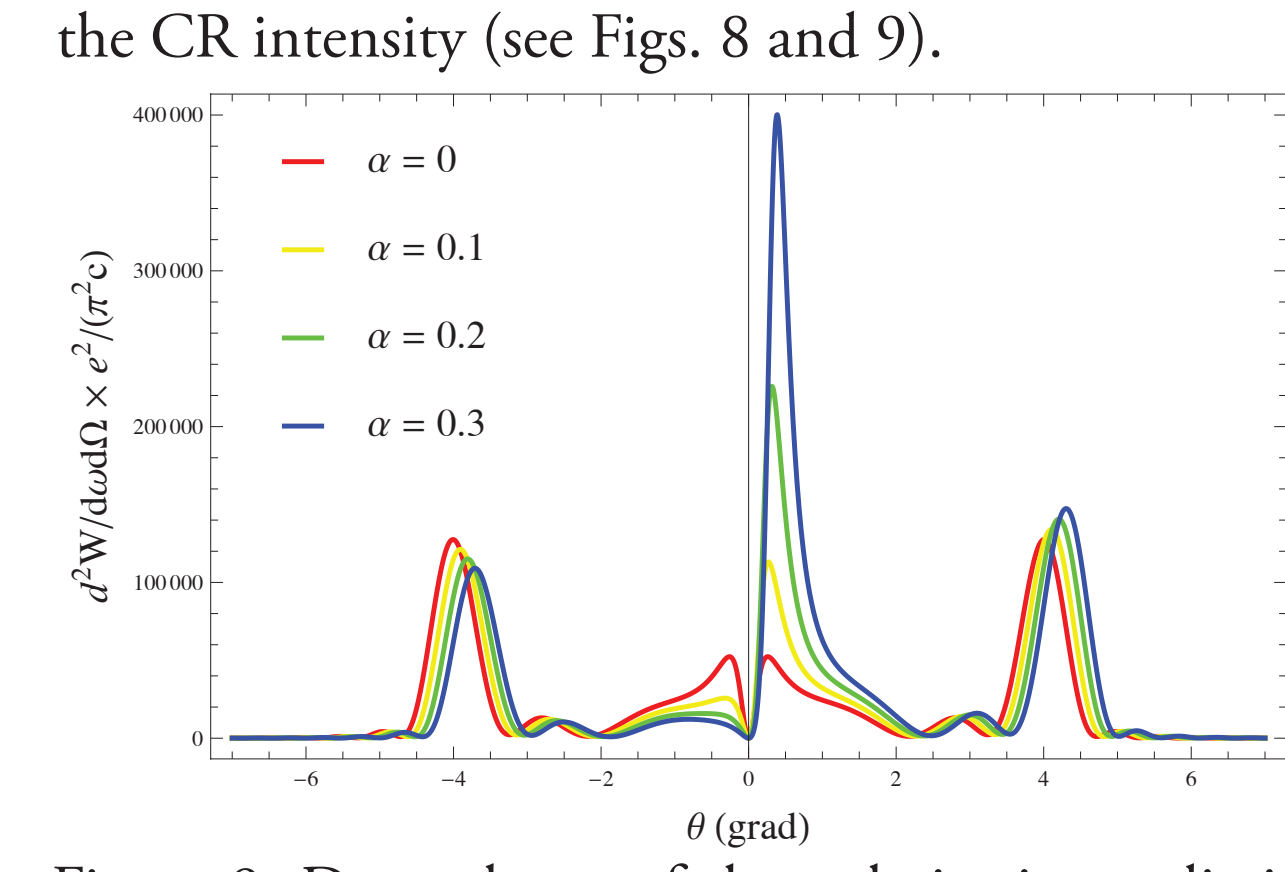


Figure 9: Dependence of the polarization radiation intensity versus the polar observation angle θ for different angles of incidence. Parameters: $\gamma = 240$, $h\omega = 284$ eV, $d = 5$ μm, $\phi = \pi$.

REFERENCES

- [1] V.A. Bazylev, V.I. Glebov, E.I. Denisov, N.K. Zhevago, and A.S. Khlebnikov, JETP Lett. 24, 371 (1976).
- [2] M.J. Moran, B. Chang, M.B. Schneider, and X.K. Maruyama, Nucl. Instrum. Methods Phys. Res. B 48, 287 (1990).
- [3] W. Knulst, O.J. Luiten, M.J. van der Wiel, and J. Verhoeven, Appl. Phys. Lett. 79, 2999 (2001).
- [4] W. Knulst, M.J. van der Wiel, O.J. Luiten and J. Verhoeven, Appl. Phys. Lett. 83, 4050 (2003).
- [5] D.V. Karlovets, JETP 136, 27 (2011).
- [6] B.L. Henke, E.M. Gullikson, and J.C. Davis, At. Data Nucl. Tables, 54, 181 (1993).